Hindawi
Geofluids
Volume 2021, Article ID 5562628, 12 pages
https://doi.org/10.1155/2021/5562628

Research Article

Study on the Permeability Change Characteristic of Gas-Bearing Coal under Cyclic Loading and Unloading Path

Fakai Wang,[1] Xuelong Li,[2,3,4] Bo Cui,[1] Jian Hao,[2] and Peng Chen[5]

[1]*College of Mining Engineering, Guizhou Institute of Technology, Guiyang, Guizhou 550000, China*
[2]*Mine Disaster Prevention and Control-Ministry of State Key Laboratory Breeding Base, Shandong University of Science and Technology, Qingdao 266590, China*
[3]*College of Energy and Mining Engineering, Shandong University of Science and Technology, Qingdao, Shandong 266590, China*
[4]*State Key Laboratory of Coal Mine Disaster Dynamics and Control, College of Resources and Environmental Sciences, Chongqing University, Chongqing 400044, China*
[5]*School of Safety Engineering, North China Institute of Science & Technology, Langfang 101601, China*

Correspondence should be addressed to Xuelong Li; lixlcumt@126.com

Received 6 January 2021; Revised 5 March 2021; Accepted 24 March 2021; Published 15 April 2021

Academic Editor: Zhigang Tao

Using the self-developed three-axis servo fluid-solid coupling system with gas-solid coupling of gas-bearing coal, the variation law of the permeability of gas coal under the stress cycle loading and unloading path was studied. The qualitative and quantitative relationships between permeability, axial force, and radial stress of gas-bearing coals were established, and the variation law of permeability of gas-bearing coals was discussed. The results show that (1) different cyclic loading and unloading stress paths correspond to the permeability characteristics of different gas-bearing coals. (2) Permeability of gas-bearing coal decreases with the increase of axial stress and radial stress, and it has a logarithmic function with axial stress and radial stress. This shows that axial stress and radial stress are important factors affecting the permeability characteristics of gas-bearing coal. (3) Under the same stress loading and unloading conditions, the axial stress is less than radial stress on the permeability of gas-bearing coal. In the cyclic loading and unloading axial stress process, the permeability of the gas-bearing coal varies by a smaller extent than the cyclically unloaded confining force. (4) The cumulative damage rate of gas-bearing coal under axial stress gradually increases with the increase of the number of cycles of loading and unloading, and the rate of the cumulative damage rate of permeability is less than the corresponding rate of radial stress.

1. Introduction

Coal is buried deep in the stratum and is a typical dual medium of pore fissures. Gas associated with it is deposited in adsorbed and free states [1]. Gas flow in the coal seam includes adsorption, desorption, diffusion, and seepage. It is a very complicated migration process. The permeability of gas-bearing coal is an important indicator of the degree of seepage of gas in the coal seam, and it is a key parameter that determines the degree of gas drainage in the coal seam.

After the coal seam is mined, the overlying strata above the coal seam are usually divided into three zones from the bottom to the top, which are the falling zone, the fissure zone, and the curved subsidence zone [2, 3]. Falling zone, which is also called goaf, are composed of irregularly broken coal and rock bodies. The vertical height can reach 4-11 times to the mining height. It has high porosity and permeability, resulting in the storage of large amounts of gas. These gasses mainly come from the adjacent fissure coal seams and rock formations [4, 5]. With the continuous mining of the working face, the coal and rock blocks in the goaf are gradually compacted due to overburden pressure and self-gravity [6]. Overburden movement and surface subsidence are caused, which may result in the destruction of buildings [7, 8]. It causes a dynamic change in the permeability of adjacent coal seams. Considering factors such as in situ stress, gas, and

physical and mechanical properties of coal, it is a hotspot and difficulty to explore the characteristics of permeability changes in gas-bearing coal seams [9].

At present, the research on the permeability characteristics of gas-bearing coal seams is mainly based on theoretical analysis, laboratory tests, and numerical simulation methods. Martin and Chandler established a relationship between damage variables and cohesion and internal friction angles by loading and unloading tests on granites [10]. Eberhardt et al. studied the effect of prepeak microcracks on macroscopic crack propagation through cyclic loading and unloading tests [11]. Xi et al. studied Young's modulus, P-wave velocity, and hysteresis loop movement with frequency variation when the loading amplitude is lower than the yield point and higher than the yield point [12]. Liu et al. studied the effect of stress amplitude and frequency on dissipative energy, dynamic elastic modulus, and dynamic Poisson's ratio under dynamic loading conditions [13].

Tian et al. carried out simulation tests on coal slag under cyclic loading and unloading under different confining forces and analyzed the macroscopic parameters, crack propagation processes, and the relationship between those under different confining forces [14]. Wang et al. conducted conventional triaxial permeation tests and controlled triaxial permeability tests with axial strain and confining force rising first and then decreased and discussed the relationship between the absolute value of the difference between the axial force and confining force and the permeability [15]. Somerton simulated the cyclic loading and unloading of particles in coal samples under different confining forces and analyzed the macroscopic parameters, crack propagation, and the relationship between them under different confining forces [16]. McKee et al. studied the relationship between stress coal porosity and permeability [17]. Harpalani studied permeability characteristics of gas-bearing coal under load conditions [18]. Enever et al. studied the effect of effective stress of coal on permeability and established the relationship between the permeability rate and effective stress [19]. Hema et al. studied the influence of the confining force on coal permeation characteristics by using carbon dioxide as seepage gas [20]. Gawuga studied the flow law of gas under coal strata under stress [21]. Sun et al. showed that the permeability and axial stress of coal samples meet the negative exponential function distribution during loading and unloading [22]. Permeability decreases during loading and recovers during unloading.

From an engineering point of view, the self-stress and tectonic stress fields with gas-bearing coal seams can be considered approximately unchanged. However, in the mining process, the disturbance generated by the production layer breaks the original stress distribution balance within the protected layer coal body. Especially, coal mine that can recover 3 layers or more. The mining process of the protected layer tends to produce cyclic stress concentration on the adjacent recoverable coal seams, resulting in the presence of stress concentration areas or stress anomalies within the adjacent coal layers of the protected layer. In high gas or gas outburst mines, mining disturbances constantly change the load of the gas-rich coal seams in the affected area, resulting in elastoplastic phenomena of gas-bearing coal seams, and this change has a significant impact on gas drainage. Бан and МаксиМОВ pointed out that the elastoplastic phenomenon has a significant influence on the seepage of coal and rock, especially for weakly cemented porous media [23]. Although many existing researches are based on the elastoplastic constitutive relation, they do not consider the effect of cyclic loading and unloading on the permeability of gas-bearing coals, essentially ignoring the irreversible deformation and permeability caused by stress cycle loading and unloading. This paper attempts to study the permeability change characteristics of gas-bearing coal under cyclic loading and unloading stress conditions to explore the infiltration rules of gas-bearing coal, in order to provide theoretical guidance for coal mine gas drainage technology.

2. Experimental Research

2.1. Experimental Principle. During the experiment, the gas flow in coal samples complies with gas seepage theory; that is, gas migration in coal seam is basically in accordance with the law of linear infiltration—law of darcy [3], and the permeability of gas containing coal gas is obtained according to the flow of the coal sample and the osmotic pressure at both ends of the coal sample. Calculate the coefficient of permeability, k, at each mean pressure, as follows: [24]

$$k = \left[(2Q_e P_e \mu \mathrm{L})/\left(P_i^2 - P_e^2\right)A\right], \tag{1}$$

where k is the coefficient of permeability, mD, Q_e is the exit flow rate of air, m^3/s, P_e is the exit pressure of air, Pa, L is the length of specimen, m, A is the cross-section area of specimen, m^2, P_i is the entrance pressure of air, Pa, and μ is the viscosity of air at temperature of test, Pa·s.

Compute the mean pressure of each test for each specimen in Pa (atmospheres) and then calculate the reciprocal of each mean pressure, as follows:

$$2/(P_i + P_e). \tag{2}$$

Plot the coefficient of permeability versus the reciprocal of the mean pressure for each test of a specimen, diagrammatic sketch as shown in Figure 1.

Draw a straight line through at least three points (this will be at the lower values of reciprocal mean pressure) and extrapolate the line to intersect the ordinate line at zero reciprocal mean pressure. The value of k at the intersection is the equivalent liquid permeability of the specimen. If a straight line cannot be established through the data points, another test at a lower mean pressure may be required, or the complete test should be repeated.

2.2. Experimental Equipment. A self-developed triaxial servo fluid-solid coupling system was employed, which allowed to test permeability under different stress conditions. The system mainly includes a confining force system with maximum loading pressure of 25 MPa, a gas supply and acquisition system with maximum supplied pressure of 6 MPa, a triaxial infiltration system with maximum pressure of 70 MPa, a gas measuring system with a measuring range of 100 sccm

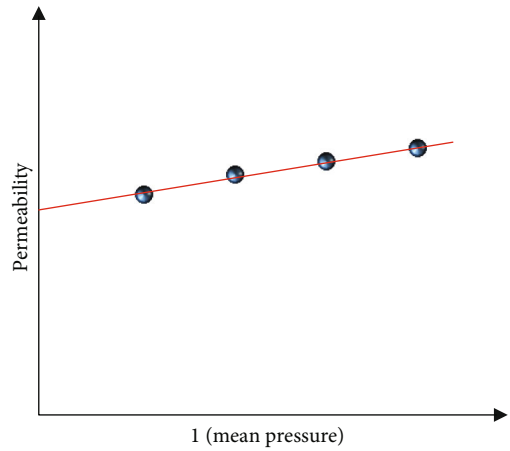

Figure 1: Permeability versus reciprocal mean pressure.

(standard-state cubic centimeter per minute), 15 slm (standard litre per minute), and 2 slm, and constant temperature water bath system with a temperature range of -25°C to 95°C. All the data in the system are automatically collected by the computer, as shown in Figure 2.

2.3. Preparation of Coal Samples. The coal samples were obtained from the Luban Northern Coal Mine (LB) of South Sichuan Coal Luzhou Co., Ltd., which is located in Sichuan Province, China. The coal mine contains several minable coal seams, whose geological conditions are simple. As shown in Figure 3, the coal samples were collected from coal seam #2 and marked as N-2, respectively. Each raw coal samples was taken from the same site and prepared according to "Methods for determining the physical and mechanical properties of coal and rock –Part 1: General requirements for sampling (GB/T23561.1-2009)" [25]. Besides, the gas pressure and the temperature of the N-2 coal seam were also measured.

The outburst danger of the N-2 coal seam of LB is evaluated in accordance with "Specification for identification of coal and gas outburst mine " (AQ1024-2006) [26] and "Prevention and Control of Coal and Gas Outburst"(2009) [27]. And, as shown in Table 1, the evaluation index test results of the N-2 coal seam were satisfy with the outburst hazard identification critical value. Then, come to the conclusion that the N-2 coal seam has the risk of coal and gas outburst.

Besides, as shown in Table 2, some of the basic parameters and proximate analysis of the N-2 coal were tested. The true relative density and the apparent relative density were measured by the MDMDY-300 automatic density instrument. Proximate analysis was determined in accordance with "Proximate analysis of coal (GB/T 212-2008)" [28]. The coal classification index (R °max) was conducted in accordance with "Method of determining microscopically the reflectance of vitrinite in coal (GB/T 6948-2008)" [29]. According to the measured parameters as shown in Table 2, it can be concluded that the N-2 coal is highly metamorphic, low-ash and low-sulfur anthracite.

In the laboratory, preparing standard coal sample is in accordance with "Method for preparation of coal sample"(GB 474-2008) [30]: firstly, selecting the large block and good integrity raw coal. Second, coring the coal sample using a Φ50 mm core barrel. Third, cutting the coal core samples into standard length using a cut machine. The standard coal samples size is Φ50 mm × 100 mm, as shown in Figure 4. Fourth, the prepared coal samples were dried and placed in a drying oven.

Due to the close wave speed characteristics of the standard coal samples, its internal crack development is similar too [31]. So, in order to avoid different crack development that affect seepage results, it is necessary to check the standard coal samples before the seepage test. Finally, using wave speed detector *HS-FSB4C* to choose the standard coal samples with close wave speed.

2.4. Experimental Procedure. The methane with a purity of 99.99% is used in the seepage test of gas-bearing coal under the cyclic loading and unloading stress path. And the experimental procedure is as follows:

(1) Apply a layer of silicone rubber about 1 mm thick on the surface of the standard coal sample

(2) The rubber sleeve, the coal sample, and the loading head are installed together on the cylindrical lower head in the sealed cylinder body of the gas seepage device, keeping the coal sample axis always perpendicular to the lower pressing head plane

(3) Tighten the external screws that seal the cylinder and check and connect all the piping and instruments

(4) Start the manual pressure pump and inject the water into the cylinder so that the true triaxial force chamber reaches the desired confining force

(5) After the confining force is stabilized, apply 2 MPa axial force to the coal sample. Then, inflate a certain pressure gas to check the airtightness of the device

(6) After passing the airtightness inspection, open the gas valve and inflate the methane with a predetermined pressure into the coal sample. After the methane flow is stabilized, record the initial gas flow

(7) After the above six steps are completed, the seepage test under the cyclic loading and unloading stress path can be performed according to Figure 5

In order to investigate the infiltration law of gas-bearing coal under the cyclic loading and unloading stress path, the following two paths were performed under the conditions of preset initial axial force σ_1 which is 2 MPa, radial pressure σ_3 which is 2 MPa, and gas pressure P which is 1 MPa. The following penetration test is as follows:

(1) Path I: keep the radial pressure σ_3 (2 MPa) and the gas pressure P (1 MPa) constant, increase the axial force σ_1 from 2 MPa step to 10 MPa, and then step down to 2 MPa, as shown in Figure 5(a)

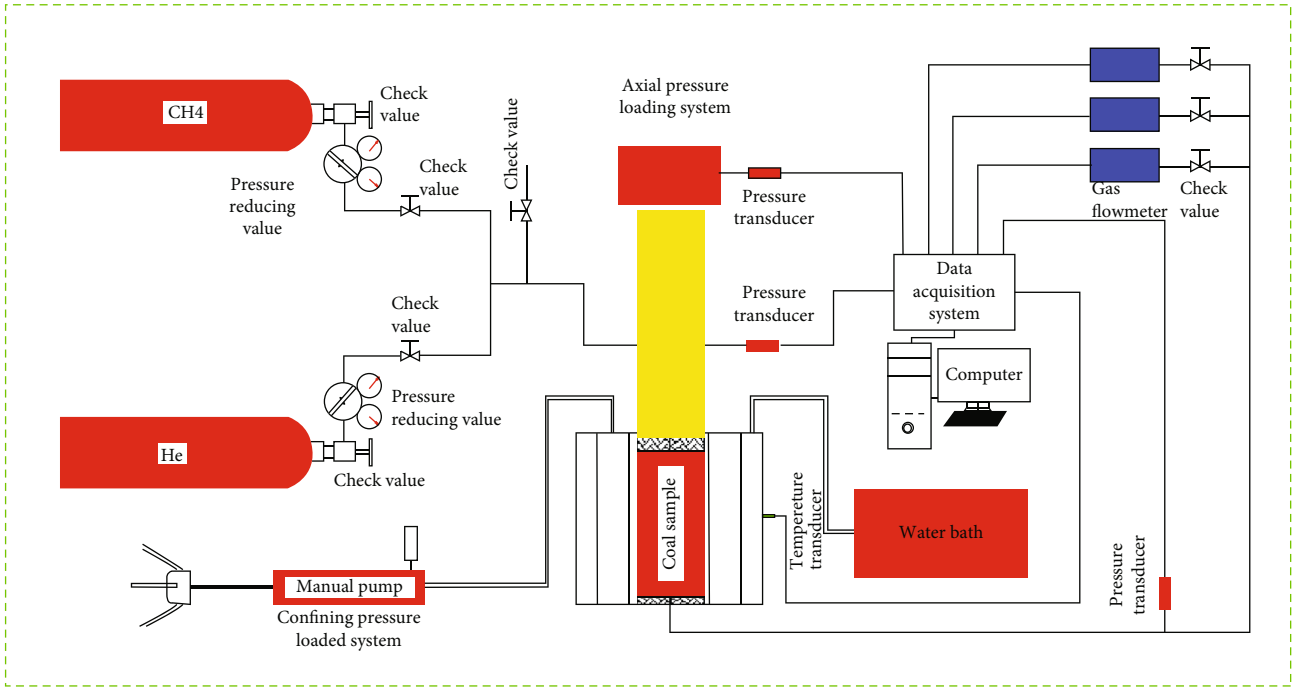

Figure 2: Sketch of the experimental system.

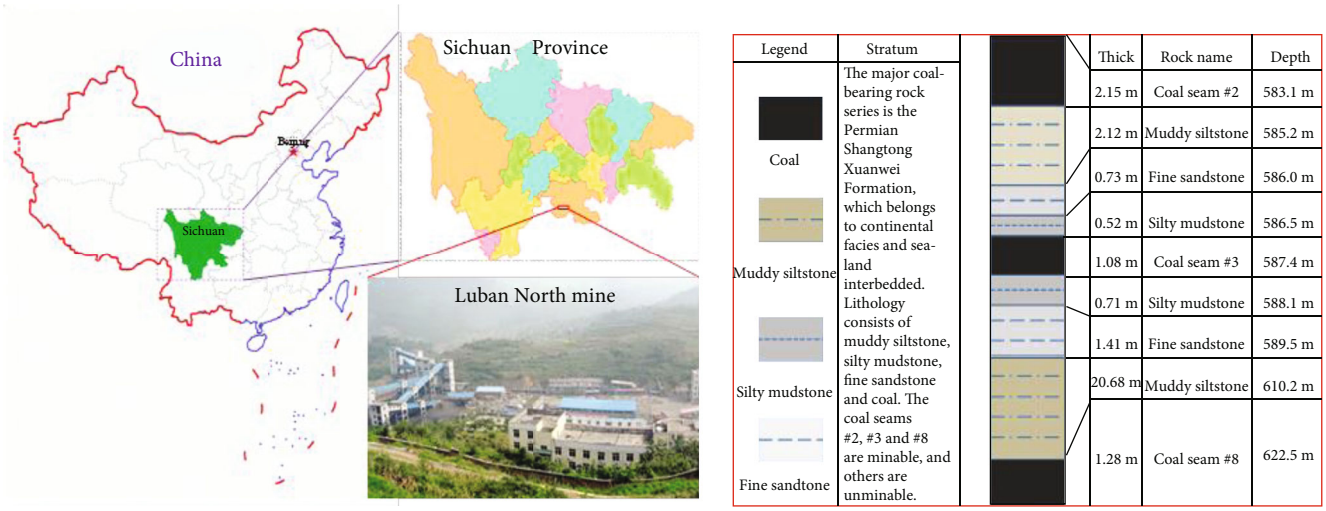

Figure 3: Location and coal seam histogram.

Table 1: Comparison between evaluation index and identification critical value.

Contents	Degree of coal fracturing	ΔP	f	P	W	T
Criteria value	III, IV, V	≥10	≤0.5	0.74	W ≥ 8	/
N-2	V	20.5	0.492	1.61	15.6377	35

P is the coal seam gas pressure, MPa; f is the coal hardiness coefficient, dimensionless; ΔP is the initial gas diffusion velocity of coal, mmHg; W is the coal seam gas content, m^3/t; and T is the coal seam temperature, °C; degree of coal fracturing is qualitative evaluation index.

(2) Path II: maintain the axial force σ_1 (2 MPa) and the gas pressure P (1 MPa) unchanged, increase the radial pressure σ_3 from 2 MPa ladder to 10 MPa, and then step down to 2 MPa, as shown in Figure 5(b).

3. Experimental Results and Data Analysis

3.1. Law of Permeability Change. According to the experimental procedure, maintain the gas pressure 1 MPa. Then, the test law of the permeability change of gas-bearing coal is carried out according to the design cyclic loading and unloading confining force path (I and II). At the end of the

Table 2: Basic parameters and Proximate analysis.

Coal seam	M_{ad}	A_{ad}	V_{daf}	$S_{t,d}$	C_{daf}	R°_{max}	TRD	ARD
N-2	1.62	9.07	6.29	0.65	92.52	3.03	1.59	1.56

Note: M_{ad} is the moisture content on air-dry (ad) basis, %; A_{ad} is the ash content on air-dry (ad) basis, %; V_{daf} is the volatile matter content on dry-ash-free (daf) basis, %; $S_{t,d}$ is the total sulfur on dry basis, %. C_{daf} is the carbon content on dry-ash-free (daf) basis, %; and R°_{max} is the vitrinite group maximum reflectance. TRD is the true relative density, g/cm^3; ARD is the apparent relative density, g/cm^3.

Figure 4: Raw coal samples.

test, the permeability of gas-bearing coal samples was calculated according to Eq. (1). The experimental results are shown in Figure 6.

Figure 6 shows the relationship between cyclic loading and unloading stress and permeability. Under the conditions of keeping the gas pressure at 1 MPa and water temperature at 35°C, the permeability of gas-bearing coal gradually decreases with the increase of the axial force and confining force, and the axial force and confining force are nonlinear. It increases with the reduction of the axial force and confining force. The axial force and confining force are both consistent with which increased nonlinear relationship. The permeability of gas-bearing coal decreases with the increase of the axial force and confining force cyclic loading and unloading, but the decreasing rate of which decreases gradually.

Under the condition that the gas pressure is maintained at 1 MPa and the water temperature is 35°C, the confining force is set to 2 MPa. According to the stress loading and unloading path I, it can be seen from Figure 6 that during the 1st cycle, the axial stress is loaded and unloaded with time. The permeability of gas-bearing coal decreased from 4.9875 mD to 3.1595 mD, and, then increased to 3.9 mD. But after recovery, the permeability value did not recover to the initial value of permeability of 4.9875 mD at the beginning of the 1st cycle loading and unloading stress. Similarly, during the 2nd and 3rd cyclic loading and unloading axial stress process, the permeability of gas-bearing coals was first decreased and then increased, but the recovery values did not return to the initial values of permeability.

Similarly, it can be seen that under the condition of maintaining the gas pressure of 1 MPa and the water temperature of 35°C, the axial force is set to 2 MPa. According to stress loading and unloading path II, it can be seen from Figure 6 that the confining force is loaded and unloaded during the 1st cycle, and the permeability of gas-bearing coal decreases first and then increases, but the value does not return to the initial permeability value of 4.8 mD. Similarly, the confining force is loaded and unloaded during the 2nd and 3rd cycles. With the increase of time, the permeability of gas-bearing coal showed a decrease and then an increase, but the increase did not return to the initial value of permeability at the beginning of the cyclic loading and unloading stress.

The variation of permeability of gas-bearing coal during cyclic loading and unloading axial stress is smaller than that of confining force. Therefore, it can be concluded that the confining force has greater influence on permeability of gas-bearing coal than the axial force.

3.2. Evolution of Permeability with the Axial Force. Under the conditions of cyclic loading and unloading stress path I, the experimental data of the coal sample permeability were fitted by regression, and the regression curve was shown in Figure 7. The optimal fitted expression formula is shown in Table 3. From Figure 7 and Table 3, it can be seen that the fitting formula is in good agreement with the experimental data, indicating that the permeability of gas-bearing coal decreases with the increase of the axial force and is a logarithmic function of the axial force.

Under the initial stress state, the permeability of coal samples varies significantly, sometimes by several times. In the process of stress loading, the permeability of coal sample decreases with the increase of axial stress. However, in the process of stress unloading, the permeability gradually recovers with the reduction of axial stress, but the closed loop curve cannot be formed, and the curves of loading and unloading do not coincide [22]. According to the research results of Li et al., the permeability of gas-bearing coal samples would tend to be constant under cyclic loading [32]. Therefore, the logarithmic function relationship should have a constant term. That is, the experimental data satisfy

$$k = a + bLn(\sigma_1), \tag{3}$$

Where a and b are all fitting constants, dimensionless.

From Table 3, it can be seen that formula (3) can well describe the variation law of gas permeability of gas-containing coal under loading and unloading axial stress path I. From Figure 7(a), it can be seen that as the axial force increases, the permeability of the coal samples decrease during the loading cycles, the permeability decrease the most during the 1st loading, and the permeability decrease the least during the 3rd loading. From Figure 7(b), it can be seen that the permeability of the coal sample increases to some extent with the decrease of the load in the axial force unloading process, the increase in the permeability of the 1st unloading process is the largest, and the 3rd unloading process penetrates. The rate of increase is the smallest.

According to the principle of effective stress proposed by Terzaghi [33], the effective stress of gas-bearing coal samples can be approximated as

$$\sigma' = \sigma - P, \tag{4}$$

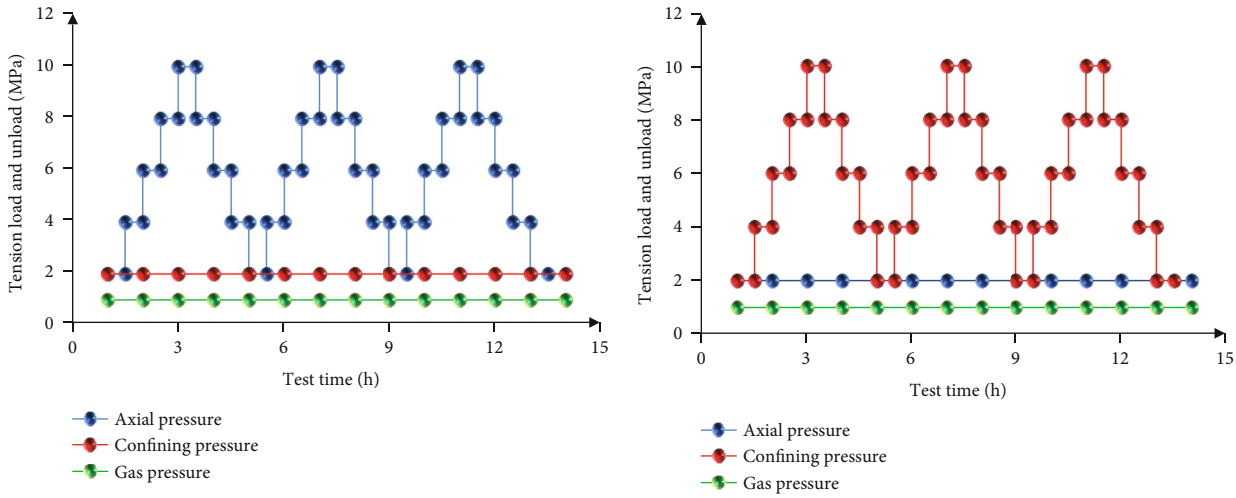

(a) Loading-unloading pass I

(b) Loading-unloading pass II

Figure 5: Circulation loading and unloading path.

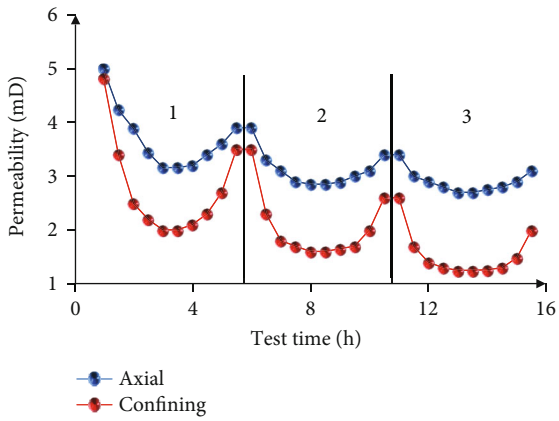

Figure 6: Experimental results under circulation loading and unloading path.

where σ' is the effective stress, and σ is the total stress of the coal sample.

According to the force state of the coal sample, it is known $\sigma_1' = \sigma_1 - P$ in the axial direction, where σ_1' is the effective stress and σ_1 is the total stress of the coal sample, respectively. It can be seen that the increase in axial stress corresponds to an increase in the axial effective stress while keeping the gas pressure constant. Therefore, the increase in effective stress causes the coal sample to be compressed more densely. The smaller pore diameter of the coal sample reduces the effective permeation path of the gas. The resistance of the migration of gas molecules is increased, and the seepage velocity of gas is reduced. As a result, the permeability of coal samples decreases, and the permeability of gas-containing coal gas decreases rapidly. This shows that coal samples are compressed and compacted under effective stress. When the force is unloaded, the effect is exactly the opposite of increasing the axial force. That is, the force unload will reduce the effective stress on the coal sample, and the reduction of the effective stress will cause the coal sample to change from compression to stress relaxation. Due to the elastic force of the coal, the pore diameter of the coal sample becomes larger. The effective percolation channel of gas is increased, and the effective percolation channel and the percolation velocity of gas are increased. This eventually led to an increase in the permeability of coal samples.

The definition of k_s is the permeability difference between the beginning and end of each loading, the format of which is $k_s = k_0 - k_t$, where k_0 is the permeability at the beginning of loading. k_t is the permeability at the end of loading. Similarly, define $k_m = |k_c - k_t|$, where k_c is the value of the permeability when the axial stress is unloaded to the initial state. One can see from the experimental results that the values of k_s and k_m gradually decrease with the increase of the cycles of loading and unloading. And Table 3 shows the values of k_s and k_m after each cycle, in which the differences between k_s and k_m for different coal samples are found to be relatively large.

It can be seen that the axial stress increases, and the permeability decreases, and when σ_1' approaches to 0, k equals to a. Thus, a can be considered as a quantity that is independent of the axial stress, and it indicates the relationship between the permeability and the coal structure. On the other hand, when σ_1' approaches to ∞, k equals to 0, which is the permeability of the coal body in no stress field. In this situation, a represents the reduced permeability, and it is due to the closure of pores and cracks when the stress field changes, that is, the permeability of the coal being affected by stress changes. The value of b reflects the stress sensitivity of the coal body, which is a scalar quantity of the changing degree of permeability when the axial stress changes, determining the changing law of the slope of the permeability curve.

3.3. Evolution of Permeability with the Confining Force. Under the condition of cyclic loading and unloading of stress path II, the experimental data of the coal sample permeability were fitted by regression. The regression fitted curve is shown in Figure 8, and the best fitting expression is shown in

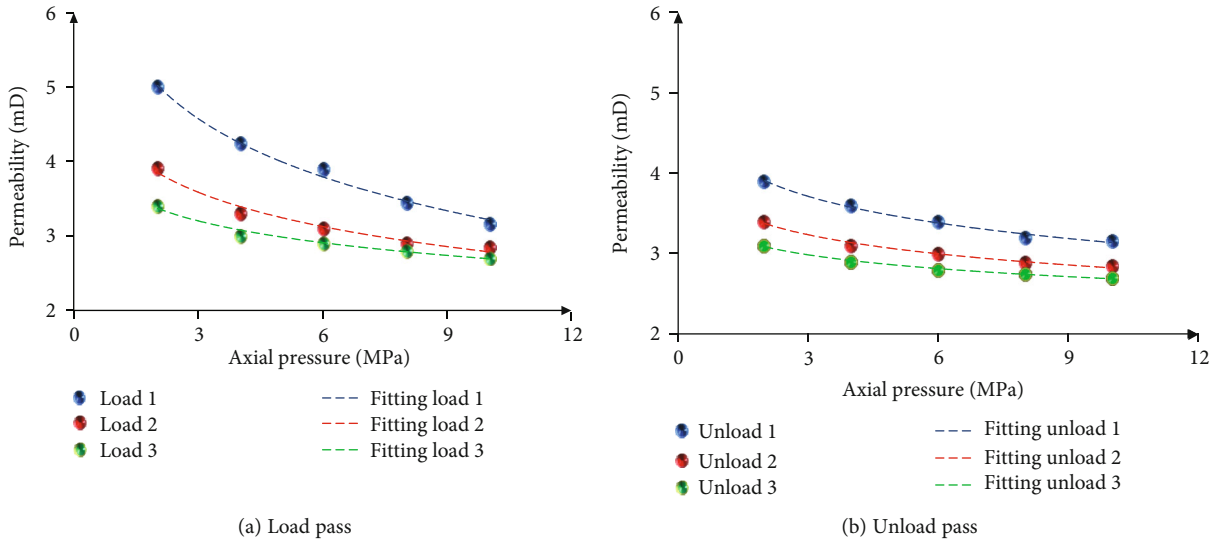

(a) Load pass (b) Unload pass

Figure 7: Permeability regression curves of coal samples under I paths.

Table 3: Regression expressions of permeability of coal samples under paths I.

Tension loading and unloading	k_m /mD	k_s /mD	Constants a	Constants b	Correlation coefficients
Load 1	/	1.83	5.7909	-1.12	0.9928
Unload 1	0.74	/	4.2429	-0.479	0.991
Load 2	/	1.05	4.3008	-0.661	0.9772
Unload 2	0.55	/	3.6145	-0.343	0.9854
Load 3	/	0.70	3.6532	-0.42	0.9758
Unload 3	0.40	/	3.259	-0.248	0.992

Table 4. From Figure 8 and Table 4, it can be seen that the fitting results are in good agreement with the experimental data. It shows that the permeability of gas-containing coal decreases with the increase of the confining force and is a logarithmic function with the confining force.

From Table 4, it can be seen that formula (3) can well describe the variation law of the permeability of gas-containing coal under loading and unloading axial stress path II. From Figure 8(a), it can be seen that as the axial force increases, the permeability of coal samples decreases during each loading cycle. The decrease in permeability was the greatest during the 1st loading, and the decrease in permeability was minimal during the third loading. As shown in Figure 8(b), it can be seen that as the load decreases, the permeability of the coal sample increases to a certain degree in the axial force unloading process. The permeability of the 1st unloading process increases the most, and the 3rd is the smallest.

When analyzing the origin of this change law, according to the effective stress principle [33], there are $\sigma_3' = \sigma_3 - P$ in radial directions, where σ_3' is the effective confining force and σ_3 is the total confining force in the radial direction of the coal sample, respectively. It can be seen that the increase in the confining force corresponds to an increase in radial effective stress. Therefore, the loading of the confining force will lead to the increase of the effective stress of coal samples. The increase of effective stress will make the coal sample be compressed more compactly, and the pore diameter of the coal sample will become smaller. The effective percolation channel of gas will be reduced, and the gas will increase. The molecular migration resistance reduces the gas flow rate of the gas and eventually results in a decrease in the permeability of the coal sample. When the confining force is unloaded, the effect is just the opposite of the effect of increasing the confining force. That is, the confining force unload will reduce the effective stress of the confining force of the coal sample, and the reduction of the effective stress will cause the coal sample to transform from compression to stress relaxation in the coal. Under the action of the elastic force, the pore diameter of the coal sample becomes larger, which increases the effective percolation channel of the gas, increases the effective percolation channel and the percolation velocity of the gas, and finally leads to the increase of the permeability of the coal sample.

Figure 8 and Table 4 show the change in permeability of the coal sample after loading under different confining forces. It can be seen that as the confining force increases, the permeability becomes smaller, and the increase in the number of loadings also makes the sensitivity of the permeability change to the confining force lower. During the unloading process, the permeability shows an increasing trend with the decrease of the effective stress. Because the pores and microcracks in the coal sample produce an irreversible deformation under the effect of effective stress, the partial permeability is irreversible after unloading.

With the radial stress increases, the permeability decreases. When $\sigma_3' \to 0$, $k = a$, where a is considered to be a quantity that is independent of the axial stress and represents the relationship between the permeability and the structure of the coal itself. When $\sigma_3' \to \infty$, the permeability

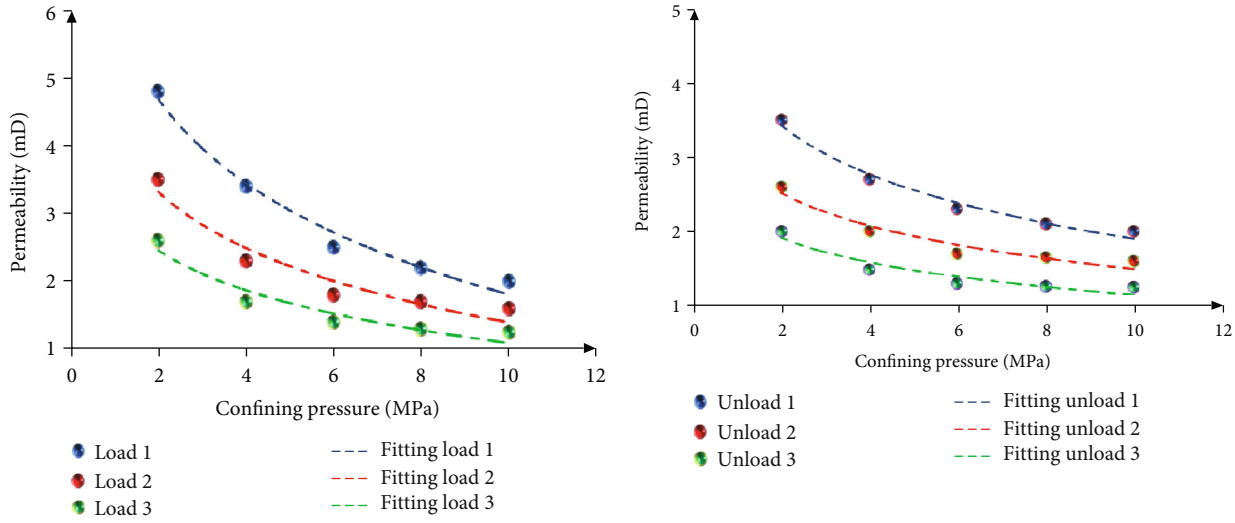

(a) Load pass II

(b) Unload pass II

Figure 8: Permeability regression curves of coal samples under II paths.

Table 4: Regression expressions of permeability of coal samples under path II.

Tension loading and unloading	k_m /mD	k_s /mD	Constants a	Constants b	Correlation coefficients
Load 1	/	2.80	5.9378	-1.792	0.9809
Unload 1	1.50	/	4.0895	-0.951	0.9816
Load 2	/	1.90	4.1553	-1.197	0.9373
Unload 2	1.00	/	2.9601	-0.636	0.9447
Load 3	/	1.35	3.0488	-0.847	0.9281
Unload 3	0.75	/	2.2446	-0.476	0.9105

$k = 0$, which is the permeability of the coal body when there is no stress field, and a reflects the part where the permeability is reduced due to the closure of pores and cracks when the permeability field changes, i.e., coal. The part of the body that is affected by stress changes. The b reflects the stress sensitivity of the coal body, which is a scalar quantity of the degree of permeability change when the axial stress changes and determines the law of the slope of the permeability curve.

4. Discussion

4.1. Effect of Effective Stress on Permeability. From the experimental data, it can be seen that the permeability and effective stress curves do not coincide during the loading and unloading process, which means that the permeability and the effective stress are not a simple function. Under cycled loading and unloading, the sensitivity of the permeability to effective stress increases with the number of loadings. Simultaneous unloading, the permeability cannot be restored to the initial value at the time of loading [14]. From the test data regression fitting results of coal sample permeability under stress path I and path II, it can be seen that the fitting result is in good agreement with the experimental data, which shows that the permeability of gas-bearing coal decreases with the increase of the axial force and confining force and with the axial force and confining force logarithmically.

According to the force state of the coal sample, there is $\sigma_1' = \sigma_1 - P$ in the axial direction, in which σ_1' is the effective stress and σ_1 is the total stress in the axial direction of the coal sample, respectively. And there is $\sigma_3' = \sigma_3 - P$ in the radial direction, where σ_3' is the confining force and σ_3 is the total confining force of the coal sample, respectively. It can be seen that the increase of axial stress corresponds to the increase of axial effective stress, and the increase of the confining force corresponds to the increase of radial effective stress. Therefore, the increase of axial stress and confining stress will increase the effective stress of the coal sample. The increase of the effective stress makes the coal sample be compressed more compactly, and the pore diameter of the coal sample becomes smaller, which reduces the effective percolation channel of the gas. The resistance to the migration of gas molecules is increased, the permeation velocity of gas is reduced, and the permeability of coal samples eventually decreases. When gas pressure is increased, the effect is just the opposite of the effect of increasing axial stress and confining force. That is, the increase of gas pressure will reduce the effective stress of the coal sample, increase the effective percolation channel of the gas, and increase the seepage velocity. This led to an increase in the permeability of coal samples [22].

With the increase of the volume stress, the absolute permeability of the coal gradually decreases, and the change is stable. This is mainly due to the increase in volume stress, making the coal more compact. The pore diameter of the coal becomes smaller, and the effective passage of gas seepage decreases. The resistance to the migration of gas molecules increases, reducing the flow rate of gas. As a result, the absolute permeability of the coal is reduced.

The experimental data of the loading and unloading path and the mathematical analysis model were fitted, and the matching degree was good. Li et al. showed that the permeability and axial stress of coal samples can form hysteresis loops under cyclic loading, which similar to the results of this study [32]. During the stress loading process, the damage of pores and cracks closed in the compaction stage on the permeability is irreparable, especially for the coal samples with low strength. At the same time, the increase in the number of loading and unloading makes the elastic properties of the coal sample stronger, and it also leads to a one-to-one correspondence between permeability and effective stress [34].

4.2. Relationship between Stress and Permeability Damage. Since the permeability rate reflects the change of effective porosity within the coal sample during the experiment, the increase of permeability indicates the increase of effective porosity, and the decrease of permeability indicates the decrease of effective porosity. Therefore, the permeability and effective porosity have the same change rule during the deformation process of coal samples. Similarly, the degree of damage to the coal sample permeability is also reflected in the porosity. That is to say, for stress paths I and II, the porosity of the coal sample also suffers damage after the stress has completed the loading and unloading cycle, and the damage rate is equal to the damage rate of the permeability [35].

Under the stress paths I and II, the two circulation axial forces and confining forces are not coincident with the permeability curves of gas-bearing coals, and the permeability of the coal samples in the force unload process is smaller than that of the loading process. That is, after the stress loading and unloading, the permeability of the coal sample cannot be restored to its original value. This shows that the permeability has been damaged to a certain extent during 1st loading and unloading stress. After 3rd of loading and unloading stress, the cumulative damage of permeability gradually increases, but the rate of damage of permeability decreases gradually.

According to the results of Jing and Yuan, the change rate of permeability and the degree of recovery of permeability can be evaluated by using the maximum permeability change rate and the damage rate of coal samples [36]. It shows that the greater the rate of change in maximum permeability, the greater the decrease in permeability of coal samples. Similarly, it shows that the greater the rate of damage in permeability, the worse the degree of recovery of permeability. The maximum permeability change rate of coal samples can be calculated as follows: [22]

$$D_{\max} = [(k_0 - k_{\min})/k_0] \times 100\%, \quad (5)$$

where $D_{\max}$ is the maximum permeability change rate of the coal sample, k_0 is the coal sample permeability measured at the first stress point during the confining force rise, and $k_{\min}$ is the coal sample permeability measured at the maximum effective stress point.

Table 5: Permeability change rate and permeability damage rate.

Tension	Loading and unloading path	$D_{\max}$ (%)	D_k (%)	D (%)
Axial force	Load and unload 1	36.65	21.8	21.8
	Load and unload 2	26.92	12.82	31.83
	Load and unload 3	20.59	8.82	37.84
Confining force	Load and unload 1	58.33	27.08	27.08
	Load and unload 2	54.29	25.71	45.83
	Load and unload 3	51.92	23.08	58.34

D is accumulated coal sample permeability damage rate, %.

The coal sample permeability damage rate can be calculated as follows:

$$D_k = [(k_0 - k_1)/k_0] \times 100\%, \quad (6)$$

where D_k is the permeation damage rate of the coal sample, and k_1 is the coal sample permeability measured at the last stress point during the confining force drop process.

According to Eqs. (5) and (6), the permeation damage rate of the gas-filled coal gas under loading and unloading under the stress paths I and II is calculated, see Table 5 for details. Under the stress path I, the maximum permeability change rate of the first cycle of loading and unloading gas-bearing coal samples was 36.65%, and the permeability damage rate was 21.8%. It can be seen that after the first stress loading and unloading cycle is completed, the permeability of the coal sample will be reduced to 78.2%. Similarly, after completing the 2nd and 3rd stress loading/unloading cycles in the axial direction, the permeability of coal samples will be reduced to 68.17% and 62.16%, respectively.

Under the stress path II, the maximum permeability change rate of the first cycle of unloading gas-bearing coal samples was 58.33%, and the permeability damage rate was 27.08%. It can be seen that after the confining force completes the 1st stress loading and unloading cycle, the permeability of the coal sample will be reduced to 72.92%. Similarly, after radial completion of the 2nd and 3rd stress loading and unloading cycles, the permeability of coal samples will be reduced to 54.17% and 41.67%, respectively.

The permeability damage rate of gas-bearing coal under various loading and unloading stress conditions is shown in Figure 9.

From Figure 9(a), it can be seen that under the condition of axial cyclic loading and unloading stress, the degree of reduction in the permeability damage rate of gas-bearing coal is the largest in the 1st cycle, and the degree of reduction in the loading and unloading stress conditions of cycles 2nd and 3rd is small. This trend of change is a macroscopic manifestation of the change in the effective stress of coal samples and the continuous expansion of internal cracks in coal samples. According to the principle of effective stress, in the stage of elastic deformation, along with the continuous increase of the axial stress of the coal sample, the internal microfissures of the coal sample are closed, and the effective seepage channel of the gas is reduced, resulting in a rapid decrease of the permeability of the coal sample. As the effective stress of

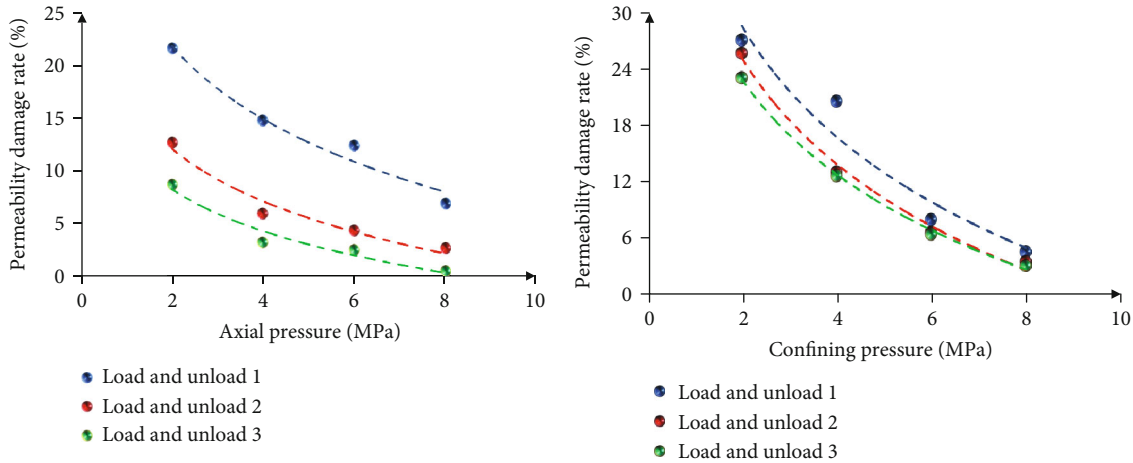

(a) Permeability damage rate under pass I

(b) Permeability damage rate under pass II

Figure 9: Permeability damage rate under cyclic loading and unloading stress.

the coal sample continues to increase, the pore diameter of the coal sample suffers from compression deformation and shrinkage, and the permeability decreases. As the effective stress of coal samples continues to increase, the pore deformation resistance and shrinkage resistance of coal mines are getting larger and larger. It shows that under the condition of cyclic loading and unloading stress, the permeability damage rate gradually decreases with the increase of loading and unloading times.

From Figure 9(b), it can be seen that under radial cyclic loading and unloading stress conditions, the degree of damage reduction of gas-bearing coal gas permeability is the highest in the 1st cycle, and the degree of reduction in the loading and unloading stress conditions of the 2nd and 3rd cycles is relatively small. This trend of change is a macroscopic manifestation of the change in the effective stress of coal samples and the continuous expansion of internal cracks in coal samples. According to the principle of effective stress, in the stage of elastic deformation, along with the continuous increase of the axial stress of the coal sample, the internal microfissures of the coal sample are closed, and the effective seepage channel of the gas is reduced, resulting in a rapid decrease of the permeability of the coal sample. As the effective stress of the coal sample continues to increase, the pore diameter of the coal sample suffers from compression deformation and shrinkage, and the permeability decreases. As the effective stress of coal samples continues to increase, the pore deformation resistance and shrinkage resistance of coal mines are getting larger and larger. It shows that under the condition of cyclic loading and unloading stress, the permeability damage rate gradually decreases with the increase of loading and unloading times.

Comparing Figures 9(a) and 9(b), under the same stress loading and unloading conditions, the axial stress is less than the radial stress on the permeability of gas-bearing coal, and the cyclic stress on gas is added under the same stress cyclic loading and unloading conditions. The coal permeability damage rate is less than radial cyclic stress. The reason for this is that the size of the coal sample used in this study is $\Phi 50 \times 100$ mm. When the axial specimen is compressed and contracted, the first internal crack closure and elastic shrinkage space are large. The 1st cyclic loading and unloading axial stress is used as the test specimen. The permeability damage rate is significantly higher than the 2nd and 3rd cycle loading and unloading axial stress. Secondly, due to the small axial stress contact area, the axial force acting on the test piece is F_A less than the radial force F_C, as shown below:

$$F_A = \pi\sigma_1 \times 25^2, \tag{7}$$

$$F_C = \pi\sigma_3 \times 25 \times 100, \tag{8}$$

where F_A is the axial force, N, and F_C is the radial force, N.

From Eqs. (7) and (8), it can be seen that when the axial stress and the radial stress are equal, the standard test piece is subjected to a radial force that is 4 times that of the axial force. Therefore, under the action of the radial force, the permeability damage rate is greater than its effect on the axial force. However, because the axial deformation space (100 mm) of the test piece is 4 times of the radial deformation size (25 mm), under the same stress, the permeability damage rate of gas-bearing coal is not 4 times an axial force under the effect of radial force. After the 1st cyclic stress is unloaded and unloaded, the permeability damage rate of gas-bearing coal under the action of axial force is 0.81 times to the radial force, and the axial force acts after loading and unloading of the 2nd cyclic stress. Under the influence of the radial force, the permeability damage rate of the lower gas-bearing coal is 0.69 times. After the 3rd cyclic stress is unloaded and unloaded, the accumulation of the permeability damage rate under the axial force is 0.65 times to the radial force. It shows that the cumulative damage rate under the axial force increases with the increase of the cycle loading and unloading times and the accumulative rate of permeability damage rate is smaller than that of radial force, that is, the axial force acts less impact on permeability than the radial force.

5. Conclusion

In this paper, an independent design of the triaxial stress system is used to design two kinds of stress loading and unloading paths. The permeability of gas-bearing coal under loading and unloading paths with axial and radial stress is measured. And the maximum permeability change rate and the permeability damage rate data are used to analysis of the experimental data. Then, explored the law of the permeability of gas-bearing coal and obtained the following conclusions:

(1) The cyclic loading and unloading stress path has an important influence on the permeability characteristics. Different cyclic loading and unloading stress paths correspond to the different permeability characteristics. The permeability decreases with the increase of axial stress and radial stress, and it changes logarithmically with axial stress and radial stress. It shows that axial stress and radial stress are important factors affecting the permeability characteristics of gas-bearing coal

(2) Under the same stress loading and unloading conditions, the axial stress is less than the radial stress on the permeability of gas-bearing coal. And the axial cyclic stress has less influence on the permeability damage rate of gas-bearing coal than the radial cyclic stress. The variation of permeability of gas-bearing coal during cyclic loading and unloading axial stress is smaller than that of radial cyclic stress. The permeability is affected by the number of cycles of loading and unloading. The degree of damage can be characterized by the maximum permeability change rate and the permeability damage rate

(3) The accumulation of the permeability damage rate of gas-bearing coal under the axial force gradually increases with the increase of the number of cycles, and the accumulative rate of the permeability damage rate is smaller than the effect of the radial force

Data Availability

The readers could obtain the data by contacting to the corresponding author.

Conflicts of Interest

The authors declared no conflicts of interest

Acknowledgments

This work is supported by the National Natural Science Foundation of China (51904167, 51474134, and 51774194), Taishan Scholars Project, Taishan Scholar Talent Team Support Plan for Advantaged & Unique Discipline Areas, State Key Laboratory of Coal Resources and Mine Safety of China (SKLCRSM19KF008), Natural Science Foundation of Chongqing, China (cstc2019jcyj-bsh0041), Postdoctoral Science Foundation Project funded by State Key Laboratory of Coal Mine Disaster Dynamics and Control (2011DA105287-BH201903), Key R&D plan of Shandong Province (2019SDZY034-2), Cultivation and Exploration and Innovation Project of New Academic Seedlings of Guizhou Institute of Technology (GZLGXM-04), and Natural Science Foundation of Hebei Province (E2019508100). We thank the anonymous reviewers for their comments and suggestions to improve the manuscripts.

References

[1] Q. Meng, L. Yan, Y. Chen, and Q. Zhang, "Generation of numerical models of anisotropic columnar jointed rock mass using modified centroidal voronoi diagrams," *Symmetry*, vol. 10, no. 11, p. 618, 2018.

[2] V. Palchik, "Formation of fractured zones in overburden due to longwall mining," *Environmental Geology*, vol. 44, no. 1, pp. 28–38, 2003.

[3] X. L. Li, Z. Y. Cao, and Y. L. Xu, "Characteristics and trends of coal mine safety development," *Energy Sources, Part A: Recovery, Utilization, and Environmental Effects*, pp. 1–19, 2020.

[4] S. M. Liu, X. L. Li, D. K. Wang, and D. Zhang, "Experimental study on temperature response of different ranks of coal to liquid nitrogen soaking," *Natural Resources Research*, vol. 30, no. 2, pp. 1467–1480, 2020.

[5] C. Ö. Karacan and K. Luxbacher, "Stochastic modeling of gob gas venthole production performances in active and completed longwall panels of coal mines," *International Journal of Coal Geology*, vol. 84, no. 2, pp. 125–140, 2010.

[6] D. M. Pappas and C. Mark, *Behavior of simulated longwall gob material. Report of Investigations/1993*, department of the Interior Bureau of Mines Ri, Pittsburgh Pa U.s, 2002.

[7] X. L. Li, S. J. Chen, Z. H. Li, and E. Y. Wang, "Rockburst mechanism in coal rock with structural surface and the microseismic (MS) and electromagnetic radiation (EMR) response," *Engineering Failure Analysis*, vol. 124, no. 6, Article ID 105396, 2021.

[8] C. Loupasakis, V. Angelitsa, D. Rozos, and N. Spanou, "Mining geohazards-land subsidence caused by the dewatering of opencast coal mines: the case study of the Amyntaio coal mine, Florina, Greece," *Natural Hazards*, vol. 70, no. 1, pp. 675–691, 2014.

[9] Z. Li, S. Liu, W. Ren, J. Fang, Q. Zhu, and Z. Dun, "Multiscale laboratory study and numerical analysis of water-weakening effect on shale," *Advances in Materials Science and Engineering*, vol. 2020, Article ID 5263431, 14 pages, 2020.

[10] C. D. Martin and N. A. Chandler, "The progressive fracture of lac du bonnet granite," *International Journal of Rock Mechanics and Mining Sciences & Geomechanics Abstracts*, vol. 31, no. 6, pp. 643–659, 1994.

[11] E. Eberhardt, D. Stead, and B. Stimpson, "Quantifying progressive pre-peak brittle fracture damage in rock during uniaxial compression," *International Journal of Rock Mechanics and Mining Sciences*, vol. 36, no. 3, pp. 361–380, 1999.

[12] Q. Meng, H. Wang, M. Cai, W. Xu, X. Zhuang, and T. Rabczuk, "Three-dimensional mesoscale computational modeling of soil-rock mixtures with concave particles," *Engineering Geology*, vol. 277, p. 105802, 2020.

[13] C. Shi, S. Wang, L. Liu, Q. X. Meng, and Q. Zhang, "Mesomechanical simulation of direct shear test on outwash deposits

with granular discrete element method," *Journal of Central South University*, vol. 20, no. 4, pp. 1094–1102, 2013.

[14] Y. Wang, B. Zhang, S. H. Gao, and C. H. Li, "Investigation on the effect of freeze-thaw on fracture mode classification in marble subjected to multi-level cyclic loads," *Theoretical and Applied Fracture Mechanics*, vol. 111, article 102847, 2021.

[15] W. Wang, L. Q. Li, W. Y. Xu, Q. X. Meng, and J. Lü, "Creep failure mode and criterion of Xiangjiaba sandstone," *Journal of Central South University*, vol. 19, no. 12, pp. 3572–3581, 2012.

[16] W. H. Somerton, I. M. Söylemezoğlu, and R. C. Dudley, "Effect of stress on permeability of coal," *International Journal of Rock Mechanics and Mining Sciences & Geomechanics Abstracts*, vol. 12, no. 5-6, pp. 129–145, 1975.

[17] C. R. McKee, A. C. Bumb, and R. A. Koenig, *Stress-dependent permeability and porosity of coal. Geology and Coal-bed Methane Resources of the Northern San Juan Basin*, Rocky Mountain Association of Geologists Guidebook, Colorado, 1988.

[18] S. Harpalani and M. J. Mcpherson, "The effect of gas evacuation on coal permeability test specimens," *International Journal of Rock Mechanics and Mining Sciences & Geomechanics Abstracts*, vol. 21, no. 3, pp. 161–164, 1984.

[19] J. R. E. Enever and A. Henning, "The relationship between permeability and effective stress for Australian coal and its implications with respect to coalbed methane exploration and reservoir model," *Proceedings of the 1997 International Coalbed Methane Symposium*, , pp. 13–22, University of Alabama, Tuscaloosa, AL, USA, 1997.

[20] H. Siriwardane, I. Haljasmaa, R. McLendon, G. Irdi, Y. Soong, and G. Bromhal, "Influence of carbon dioxide on coal permeability determined by pressure transient methods," *International Journal of Coal Geology*, vol. 77, no. 1-2, pp. 109–118, 2009.

[21] J. Gawuga, *Flow of gas through stressed carboniferous strata, [Ph.D. thesis]*, University of Nottingham, Nottingham, 1979.

[22] L. Yang, W. Xu, Q. Meng, and R. Wang, "Investigation on jointed rock strength based on fractal theory," *Journal of Central South University*, vol. 24, no. 7, pp. 1619–1626, 2017.

[23] А. Бан and В. А. Максимов, *The influence of rock properties on liquid flow underground*, Z. Zhaochen, Ed., Petroleum Industry Press, Beijing, 1981.

[24] "Standard test method for permeability of rocks by flowing air. Designation: D 4525 - 90, Reapproved," 2001.

[25] "Methods for determining the physical and mechanical properties of coal and rock - part 1: general requirements for samplingNational standards of People's Republic of China, GB/T 23561.2009.

[26] "Specification for identification of coal and gas outburst mine-People's Republic of China safety production industry standards, AQ 1024-2006.

[27] "Prevention and control of coal and gas outburst," People's Republic of China State Administration of Work Safety, 2009.

[28] "Proximate analysis of coal. National standards of People's Republic of China, GB/T 212-2008".

[29] "Method of determining microscopically the reflectance of vitrinite in coalNational standards of People's Republic of China, GB/T 6948-2008.

[30] "Method for preparation of coal sampleNational standards of People's Republic of China, GB 474-2008.

[31] Q. Wu, H. Li, and J. Yang, "Discussion on the variation and quantification of penetrating signal waveform in acoustic wave detection," *Geophysical & Geochemical Exploration*, vol. 36, no. 1, pp. 144–148, 2012.

[32] X. Li, G. Yin, and B. Cai, "Experimental study of deformation and seepage properties of outburst coal samples under cyclic loading," *Chinese Journal of Rock Mechanics and Engineering*, vol. 28, no. 2, pp. 3498–3504, 2009.

[33] K. Terzaghi, *Theoretical soil mechanics*, John Wiley & Sons Inc., New York, 1943.

[34] X. M. Zhang, D. M. Zhang, C. J. Leo, G. Z. Yin, D. Feng, and D. S. Liyanapathirana, "Damage evolution and post-peak gas permeability of raw coal under loading and unloading conditions," *Transport in Porous Media*, vol. 117, no. 3, pp. 465–480, 2017.

[35] D. K. Wang, *Research on constitutive models and instability rules of gas-saturated coal, [Ph.D. thesis]*, Chongqing University, Chongqing, 2009.

[36] Y. Lin, Y. Qin, D. Ma, and J. Zhao, "Experimental research on dynamic variation of permeability and porosity of low-rank inert-rich coal under stresses," *ACS Omega*, vol. 5, no. 43, pp. 28124–28135, 2020.